Results from a new reticle defect inspection platform

William H. Broadbent*, James N. Wiley, Zain K. Saidin, Sterling G. Watson,
David S. Alles, Larry S. Zurbrick, Chris A. Mack
KLA-Tencor Corporation, 160 Rio Robles, San Jose, CA, USA 95134-1809

ABSTRACT

A new DUV high-resolution reticle defect inspection platform has been developed to meet the sub-90nm node 248/193nm lithography reticle qualification requirements of the IC industry. This advanced lithography process typically includes COG layers, EPSM layers, and AltPSM layers; aggressive OPC is typically used which includes jogs, serifs, and SRAF (sub-resolution assist features). The architecture and performance of the new reticle defect inspection platform is described. Die-to-die inspection results on standard programmed defect test reticles are presented showing typically 50nm edge placement defect sensitivity, 80nm point defect sensitivity, 5.5% flux defect sensitivity, and 100nm quartz phase defect sensitivity. Low false detection results are also shown on 90nm node and below product reticles. Direct comparisons with UV wavelength inspections show measurable sensitivity improvement and a reduction in false detections. New lithography oriented defect detectors are discussed and data shown.

Keywords: DUV, 193nm, 248nm, reticle, defect, inspection, sensitivity, flux, OPC, SRAF

1. Introduction

The current generation of reticle defect inspection systems have provided excellent performance for current IC manufacturing down to the 130nm node. Using high resolution imaging and UV wavelength illumination, these systems have been effective in finding critical reticle defects during reticle manufacturing, and further, finding critical reticle defects that occur during reticle use, thus protecting wafer fabs from catastrophic yield losses. UV illumination has been effective for both 365nm and 248nm wavelength lithography.

These UV systems have been extended in use to the 90nm node, however, the lower k_1 and 193 lithography of the 90nm node are demanding detection of smaller defects on smaller feature sizes and challenging these systems. Futhermore, local CD defects and crystal type defects have been problematic in some advanced wafer fabs. The newly developed DUV reticle inspection platform uses DUV illumination for higher imaging resolution, thus allowing inspection of smaller feature sizes and detection of smaller defects. In addition, the platform has been designed with sufficient resolution for extension to the 65nm node and possibly beyond. Finally, the platform design includes the necessary inspection modes, illumination modes, and detection algorithms suitable for the variety of aggressive OPC and phase shifting techniques anticipated for the 65nm node.

Factory test results from the die-to-die transmitted illumination prototype and the first two beta systems are discussed, including some comparisons to the current generation UV system.

Discussion and early test results from the new lithography oriented defect detectors are also presented. These detectors are designed to offer variable detection sensitivity according to the local mask enhancement factor (MEF), thus, defects in high MEF locations are detected with very high sensitivity, whereas, defects in low MEF locations are detected with lower sensitivity. When used in conjuction with the traditional high resolution detectors, defects can be binned as either lithographically significant or not lithographically significant.

2. DUV Reticle Inspection Development

KLA-Tencor is currently in development of the DUV TeraScan platform. This advanced DUV platform is being designed to include a die-to-die inspection mode, a die-to-database mode, and a STARlight™ contamination mode. The TeraScan 525 die-to-die model (see Figure 2-1) has recently finished factory testing, and two beta systems have been shipped for field testing - one system is currently in production while the other is finishing installation. The die-to-database mode is currently starting the factory testing cycle, while the STARlight capability is being designed.

* bill.broadbent@kla-tencor.com; phone 408-875-6153; fax 408-875-4262

Proceedings of SPIE Vol. 5256 23rd Annual BACUS Symposium on Photomask Technology,
edited by Kurt R. Kimmel, Wolfgang Staud (SPIE, Bellingham, WA, 2003) · 0277-786X/03/$15.00

Downloaded From: http://proceedings.spiedigitallibrary.org/ on 05/06/2014 Terms of Use: http://spiedl.org/terms

The TeraScan platform continues KLA-Tencor's tradition of high resolution imaging for high performance reticle inspection. This technique uses significantly higher resolution imaging of the reticle than the wafer lithography system thus allowing direct inspection of both the primary structures and the sub-resolution structures to ensure a high quality reticle. Furthermore, since the inspection is done at high resolution, a single wavelength system can provide good performance inspecting reticles from a variety of lithographic wavelengths.

Figure 2-1: TeraScan 525 DUV Reticle Inspection System

Since different defects may be significant to different groups of reticle parties, KLA-Tencor is developing image processing algorithms to bin defects according to their significance. For instance, small defects on large geometry or on sub-resolution assist features (SRAF) may have little lithographic significance since the MEF is low, so they may not be important to a lithographer. However, these defects can be important to the reticle manufacturer for process control as an indication of process quality. A high resolution inspection system has the ability to image many types of defects, and with appropriate image processing, can bin different defect types.

The TeraScan platform has been designed for production reticle inspection of 248nm and 193nm wavelength reticles for the 90nm node including typical binary (COG), EPSM, and dark field alternating PSM. Capability extensions are in development for 65nm node production reticles including more aggressive RET, such as tri-tone, chromeless, etc. Finally, the system is being designed with capability for the development of 157nm wavelength and EUV reticles for lithography below the 65nm node.

3. Technology

3.1. Image Acquisition

A simple block diagram of the DUV TeraScan image acquisition subsystem is shown in Figure 3-1. It uses a high resolution microscope and linear sensor architecture, as opposed to the multi-beam laser scanner architecture of the current generation UV TeraStar system. The TeraScan architecture offers several advantages to the laser scanner which include the potential for higher speed in the future, and no beam crosstalk.

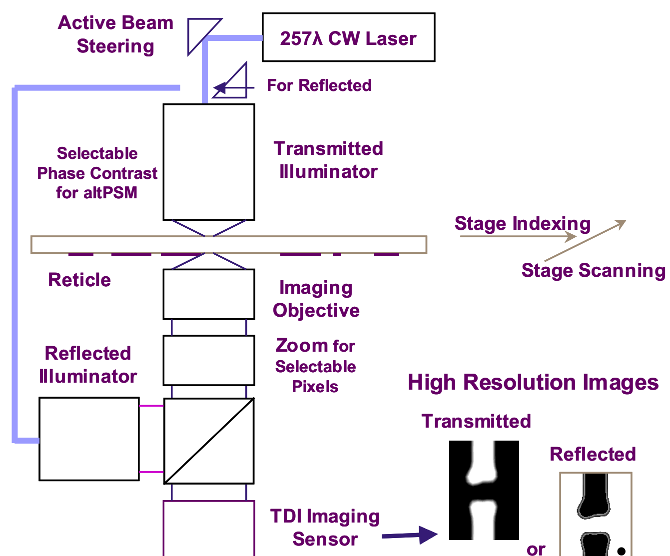

Figure 3-1: TeraScan High Resolution Image Acquisition Subsystem Block Diagram

Referring to the top of the diagram, the illumination source is a 257nm wavelength continuous wave (CW) laser. There is an active beam steering subsystem to compensate for beam drift and to reduce laser replacement time. The transmitted light illuminator has several different configurations that can be selected by the user at run-time. Two configurations are currently implemented: standard contrast for binary and EPSM reticles, and phase contrast for quartz etch reticles such as alternating, chromeless, etc. The phase contrast mode provides improved imaging contrast to quartz phase defects (bumps and divots) allowing higher defect sensitivity.

Downloaded From: http://proceedings.spiedigitallibrary.org/ on 05/06/2014 Terms of Use: http://spiedl.org/terms

The reticle is inspected with the pattern surface down. The air bearing stage scans the reticle in one axis for continuous image pick-up, and then indexes in the other axis after each swath to provide a serpentine inspection path.

The custom designed objective images the reticle surface through the zoom lens onto the imaging sensor. The zoom lens allows different pixel sizes to be selected by the user at run-time providing different defect sensitivities and associated scan times - currently a 125nm pixel size is implemented with 90nm and 175nm pixels in development. Image pick-up is done with a time-domain-integration (TDI) sensor. This sensor design offers high speed continuous image pick-up at much lower light levels than a conventional CCD linear sensor.

The system also includes a reflected illumination optical path which is currently used during defect review to aid in the correct classification of contamination. Inspection with reflected illumination is currently in development for die-to-die, die-to-database, and STARlight modes.

At the bottom of Figure 3-1, the high resolution images show transmitted and reflected images of a binary reticle. Note that the sub-resolution clear serifs are imaged and clearly visible thus allowing defects on the serifs to be readily detected. An oversize clear serif defect is present and visible in both the transmitted and the reflected images, however, a particle on the dark material is also present but is only visible in the reflected light image.

As with lithography systems, slight amounts of mechanical or optical error will reduce overall system performance. Since high sensitivity die-to-database inspection is the most demanding of the three applications, the optical and mechanical tolerances of the platform are determined by this mode. To allow a future upgrade to die-to-database mode, the 525 die-to-die system was designed with the very tight tolerances required for die-to-database mode.

3.2. Image Processing

Figure 3-2 shows a simple block diagram of the TeraScan image processing subsystem. The Tera Image Supercomputer is a fully programmable and scalable multi-processor architecture. This image computer is very similar to the TeraStar image computer but can be configured with more processors and memory for additional speed and algorithm complexity.

The transmitted or reflected image stream is stored in the Optical Image Memory; several swaths are buffered to allow variable processing rates according to geometry density thus improving the overall speed. Sophisticated alignment and detection algorithms are executed in the Defect Detection block to provide both high sensitivity and binning by defect type. The basic detection method is to overlay a test image with a matching reference image and look for differences above a pre-selected size - any differences are the result of a defect. For die-to-die inspection, the test and reference images compared are from adjacent die; for die-to-database inspection, the reference image is reconstructed from the database. For STARlight inspection, the transmitted and reflected images of the same geometry are compared. In Figure 3-2, note that the Test and Reference images are the same except for the oversize serif. In the difference image (overlay), everything matches except the oversize serif which is represented as a bright spot that the defect detectors can identify.

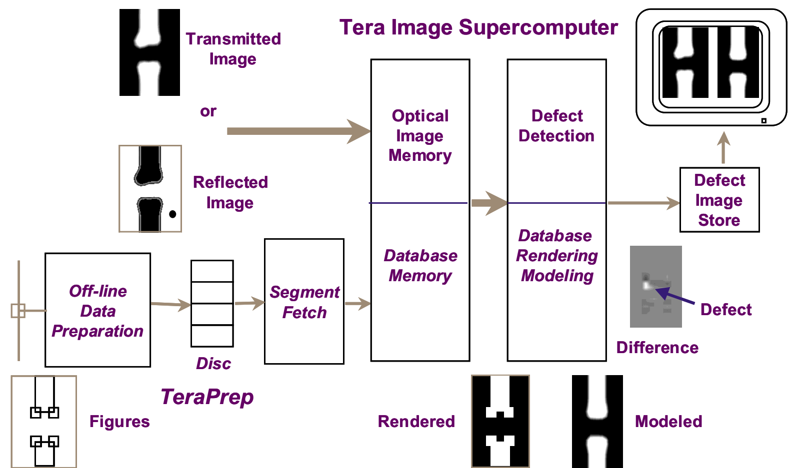

Figure 3-2: TeraScan Image Processing Block Diagram

The processing blocks for die-to-database inspection are shown in italics in the lower part of Figure 3-2 since they are currently in development. These processing blocks construct a matching image in real time from the database used to

Downloaded From: http://proceedings.spiedigitallibrary.org/ on 05/06/2014 Terms of Use: http://spiedl.org/terms

write the reticle. Starting from the left side of Figure 3-2, an off-line data preparation operation is performed to optimally organize and format the input database figures for inspection (rather than for design or writing). This step is done off-line and the inspection-ready file is stored on the high speed disc. At runtime, as the optical system is scanning the reticle, the Segment Fetch block selectively accesses the appropriate figure segments of the database for the current swath and stores them in the Database Memory. As each geometry is processed for defect detection, the database figures are rendered (figures placed in the correct locations and interior lines removed), and then modeled to match the optical image. Sophisticated modeling algorithms must be used to ensure that that database image exactly matches the optical image - any error creates noise and reduces defect detection sensitivity.

The database processing blocks are basically the same as for the current TeraStar system, however, TeraScan can be configured with additional processing speed and capacity for the anticipated larger databases of the advanced nodes. Moreover, TeraScan has more sophisticated modeling capability to provide high sensitivity for the more aggressive OPC and phase shifting designs of the advanced nodes.

3.3. Image Acquisition Cut-away

A cut-away illustration of the Image Acquisition Subsystem (IAS) is shown in Figure 3-3. In addition (not shown), there is a separate utilities module (must be located nearby), image computer rack, and data preparation rack (both racks can be remotely located).

Referring to Figure 3-3, the Stage is in the middle, the Transmitted Illuminator is above, while the Optics Bench is below (contains the objective, zoom, sensor, and reflected illuminator). Reticles are loaded and unloaded from the front via either a Manual Load Port for unboxed reticles, or the SMIF Load Port (both can be installed simultaneously). A reticle library is included inside for queued operation. The stand-alone operator console can be located nearby.

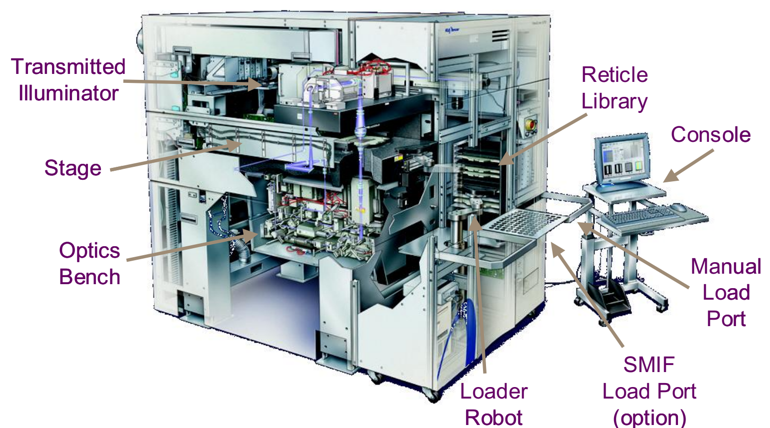

Figure 3-3: TeraScan Image Acquisition Subsystem Cut-away

4. Test Results

The TeraScan 525 die-to-die system recently completed 6 months of testing and tuning (January to June 2003) prior to the start of Beta testing. The 6 months of testing consisted of the final phase of Engineering Test, all of Alpha Test, and Source Acceptance of the first two beta systems. Three systems were used for the testing to allow for a first look at system-to-system variation - the prototype and the first two beta systems. The 125E pixel in die-to-die transmitted illumination was used for all of the testing.

KLA-Tencor uses five standard reticle designs for sensitivity and false detection testing. Several reticles of each type were used to allow a first look at reticle-to-reticle variation. Selected performance data is shown in the sections below.

In addition to the standard reticles, KLA-Tencor received approximately sixty reticles from the industry to include in the testing; they included a variety of reticle types, writer types, manufacturers, geometry designs, and defect types.

Of the sixty reticles, approximately fifty were 90nm node, both 248 and 193 lithography, while approximately ten were 193 lithography development reticles for the sub-90nm nodes. The fifty 90nm node reticles included binary, EPSM (6%, 9%, 18%), and dark field alternating PSM. Of the total, approximately forty were critical product layers, while approximately ten included programmed defects.

Downloaded From: http://proceedings.spiedigitallibrary.org/ on 05/06/2014 Terms of Use: http://spiedl.org/terms

Overall, the testing showed that the system met its target performance level for sensitivity, inspectability, and false detections with no major issues - some minor issues were identified and are being corrected.

4.1. KLA-Tencor Test Reticle Die-to-die Results

Figure 4-1 shows the sensitivity performance in die-to-die mode using the KLA-Tencor Spica-400-193 test reticle and the 125E pixel. This test reticle is standard 6% EPSM for 193 lithography and includes the semi-wire programmed defect test section with approximately 450nm dark lines (shown). This result was taken from Beta1 using the 125E pixel, and standard high resolution detectors (HiRes) at maximum sensitivity. Each gray box indicates 100% detection of 20 contiguous inspections. The number in the gray boxes is the defect size using the KLA-Tencor maximum inscribed circle (MIC) method from SEM images. The red line indicates the specified performance level which was met by the system - note that there is no specification for spot defects due to the difficulty in repeatably manufacturing them. Similar results were obtained using the binary and 248 versions of this test reticle. Also, very little system-to-system, reticle-to-reticle, and day-to-day variation was observed (data not shown).

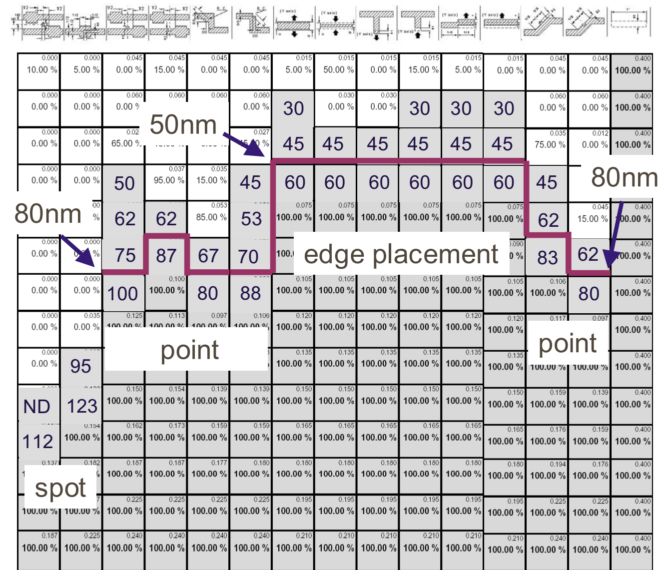

Figure 4-1: Die-to-die Sensitivity from Spica-400-193 EPSM

Figure 4-2 shows the defect images from a typical die-to-die inspection report for a 30nm oversize CD defect. The gray scale Test and Reference images are shown with the Edge Enhance feature enabled (green and magenta figure outlines). Note that this defect cannot be correctly classified by simply visually comparing the Test and Reference images, whereas, the defect is easily visible in the Difference Image as the dark outline (mismatch between Test and Reference). The operator can further measure the defect using the Linewidth Measuring review tool (not shown). The inspection map is also shown where each colored dot is a detected defect. Note the many off grid defects which are naturally occurring defects that were detected.

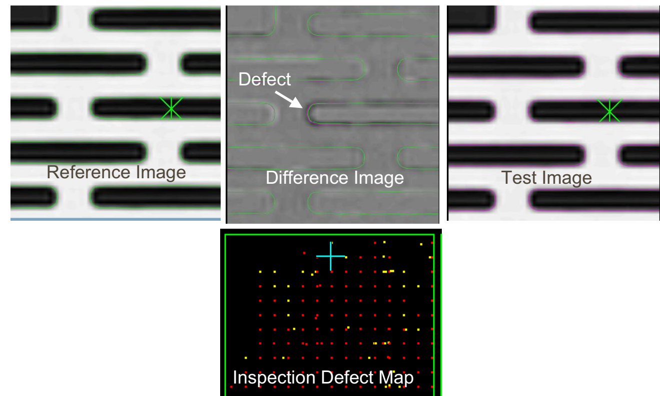

Figure 4-2: 30nm Oversize CD Defect from Spica-400-193

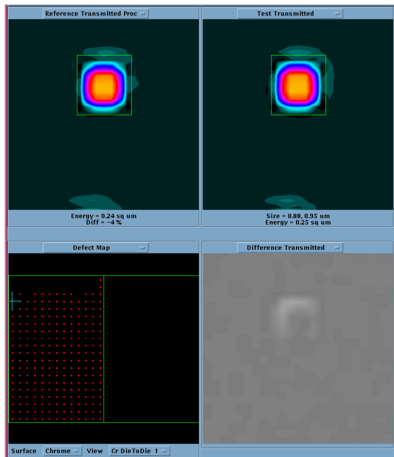

Figure 4-3 shows a 4% contact flux defect from the Cetus-600-248 test reticle. This reticle has programmed oversize and undersize contacts from approximately 1% to 30% error by area which closely correlates with flux. The nominal contact size is 600nm in both dense (1:3) and isolated arrays. This particular inspection was done with the new high sensitivity flux detector (Litho2). A sensitivity chart is not shown, however, the system performance meets the specified 5.5% flux undersize and 8% flux oversize requirement on both the 248 and 193 lithography 6% EPSM Cetus reticles.

Figure 4-3: Die-to-die 4% Contact Flux Defect from Cetus-600-248

Downloaded From: http://proceedings.spiedigitallibrary.org/ on 05/06/2014 Terms of Use: http://spiedl.org/terms

Figure 4-4 shows typical quartz bump defect detection performance on the Dione-280-193 test reticle. This test reticle is a dark field alternating design with 280nm linewidths and an etch depth for 193 lithography; it contains chrome, quartz bump, and quartz divot defects, in both shifted and unshifted areas. Figure 4-4 shows 180º, 120º, and 60º quartz bumps in a 180º well which is typically the most lithographically significant situation. The defect sizes are using the KLA-Tencor MIC method from SEM images. The green bars are 100% detection (20 runs) using standard contrast and focus, while the blue bars used the phase contrast mode and off-focus for better sensitivity (TeraPhase 501). Note that the phase contrast mode provides significantly better performance for the shallower defects.

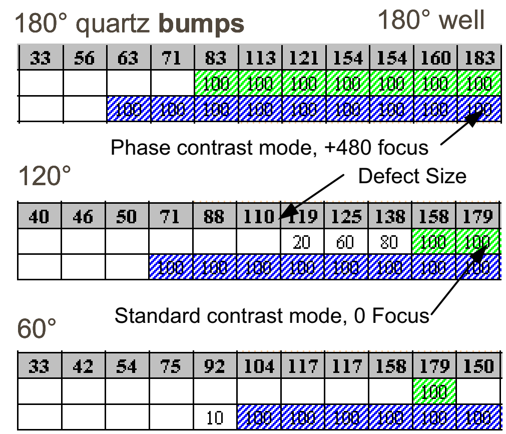

180° quartz **bumps** 180° well

33	56	63	71	83	113	121	154	154	160	183
				100	100	100	100	100	100	100
		100	100	100	100	100	100	100	100	100

Phase contrast mode, +480 focus

120° Defect Size

40	46	50	71	88	110	119	125	138	158	179
						20	60	80	100	100
			100	100	100	100	100	100	100	100

Standard contrast mode, 0 Focus

60°

33	42	54	75	92	104	117	117	158	179	150
									100	
				10	100	100	100	100	100	100

Figure 4-4: Die-to-die 193 Quartz Bump Performance from Dione-280-193

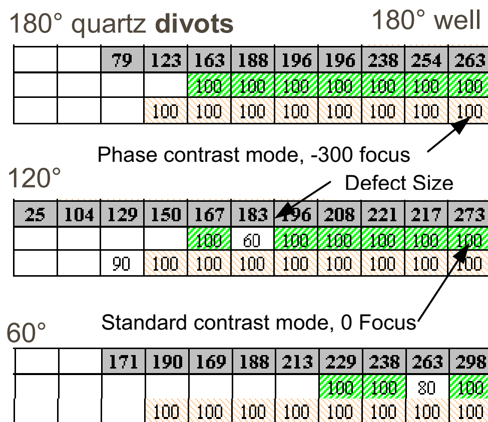

180° quartz **divots** 180° well

		79	123	163	188	196	196	238	254	263
				100	100	100	100	100	100	100
			100	100	100	100	100	100	100	100

Phase contrast mode, -300 focus

120° Defect Size

25	104	129	150	167	183	196	208	221	217	273
				100	60	100	100	100	100	100
		90	100	100	100	100	100	100	100	100

Standard contrast mode, 0 Focus

60°

		171	190	169	188	213	229	238	263	298
							100	100	80	100
			100	100	100	100	100	100	100	100

Figure 4-5: Die-to-die 193 Quartz Divot Performance from Dione-280-193

Figure 4-5 shows typical quartz divot defect detection performance. Negative focus was chosen which provides the best detection for divots vs. positive focus for the bumps. While overall best performance for a finished alternating reticle might require three passes (positive focus, zero focus, and negative focus), a more economical alternative is to only do a positive focus pass after the quartz etch, skipping the negative focus pass since divot defects are very rare, and further skipping the zero focus pass for chrome defects which were found in the standard pass before the quartz etch.

4.2. Recent Testing

During the months of July and August 2003, additional testing was done using the new 125 and 90 pixels, and also, early testing with die-to-database mode. The new 125 and 90 pixels were designed for die-to-database mode to provide both higher sensitivity for the 65nm node (90 pixel), and also lower noise for better die-to-database performance versus the existing 125E pixel. The new pixels are also planned for die-to-die mode, with 125 replacing 125E.

Also being tested are the first articles of smaller linewidth and smaller defect size reticles which are more suitable for the 65nm node (reticles from several manufacturers).

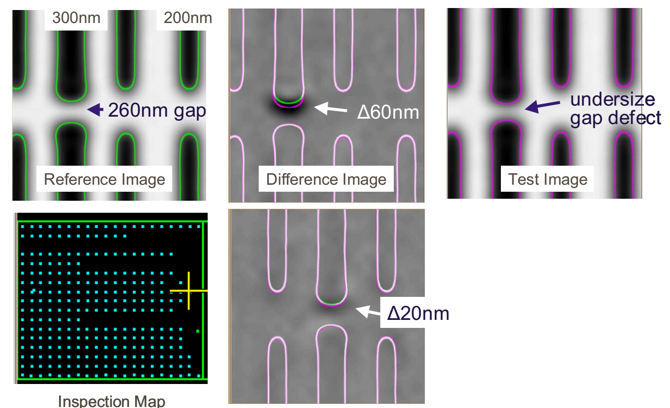

Figure 4-6: Gap Defects with 90 Pixel Die-to-die from Spica-300-193

Figure 4-6 shows defect images from the new 90 pixel in die-to-die mode using the new Spica-300-193 EPSM reticle. This is a shrink of the previous Spica and has approximately 300nm primary lines. The section

Downloaded From: http://proceedings.spiedigitallibrary.org/ on 05/06/2014 Terms of Use: http://spiedl.org/terms

shown is the OPC6 section with approximately 200nm wide SRAF. Two defects are shown, the upper one is a 60nm undersize gap, the lower one is 20nm. Note that there is just one off-grid naturally occurring defect even at this very high sensitivity level suggesting a well controlled reticle manufacturing process.

Figure 4-7 shows early die-to-database results with the new 125 pixel. This data was taken with the Spica-400-193 reticle (semi-wire pattern) using the HiRes detectors at maximum sensitivity. Note that the performance meets the target sensitivity specification (same as die-to-die), although there is slightly less margin than with die-to-die.

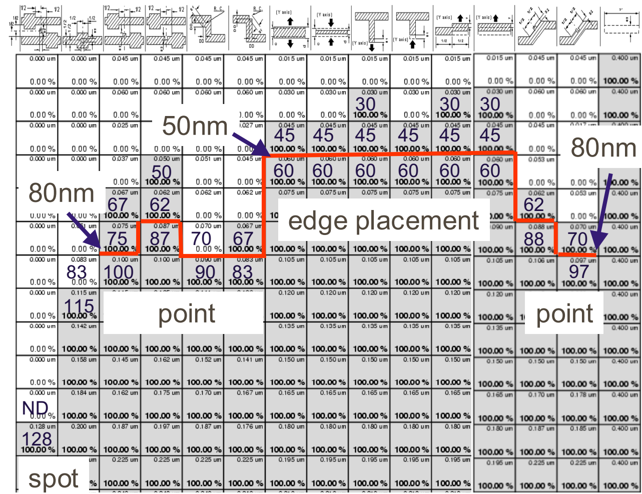

Figure 4-7: Early Die-to-database Sensitivity with 125 Pixel from Spica-400-193

Figure 4-8 shows a 45nm undersize CD defect detected in die-to-database mode with the new 125 pixel. This data was taken with the Spica-400-193 reticle (semi-wire pattern) using the HiRes detectors at maximum sensitivity.

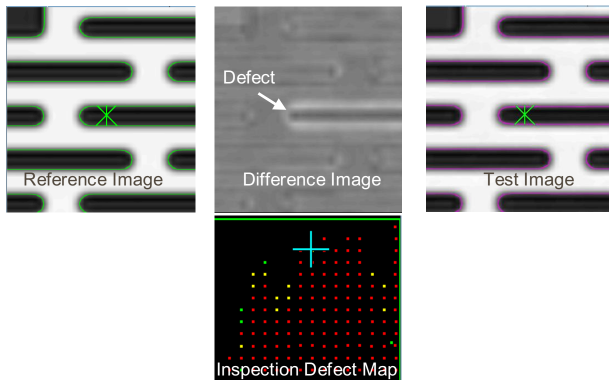

Figure 4-8: 45nm CD Defect - Early Die-to-database result with 125 Pixel from Spica-400-193

4.3. Industry Product Reticle Results

As discussed in Section 4.1, approximately sixty reticles were provided by the industry for die-to-die testing. Many reticle manufacturers and wafer fabs provided the reticles. The results from selected reticles are shown here.

Figure 4-9 shows an 8% flux undersize contact detected by the high sensitivity flux detector (Litho2) using the 125E pixel in die-to-die mode. The reticle is a 90nm node 6% EPSM for 193 lithography and is a product contact layer. The contacts are approximately 600nm on a 1:1 pitch.

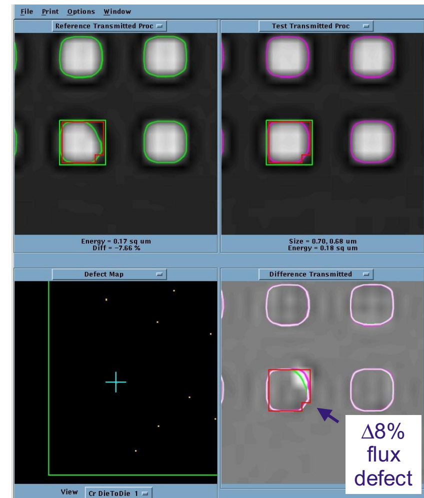

Figure 4-9: 8% Flux Defect Detected with 125E Litho2 Die-to-die - 90nm Node 193 EPSM Contact Layer

Downloaded From: http://proceedings.spiedigitallibrary.org/ on 05/06/2014 Terms of Use: http://spiedl.org/terms

Several 90nm node 6% EPSM product simulation reticles for 193 lithography were provided by the Advanced Mask Technology Center (AMTC - Dresden, Germany). Each reticle was first inspected by an SLF27 at maximum sensitivity with the 150 pixel in die-to-die mode - a few small defects were typically detected. The reticles were then inspected with the higher sensitivity 525 125E pixel, first at maximum sensitivity which resulted in far too many defects, then a reduced sensitivity setting was selected that found a manageable number of defects (<100). Although the defects were small, a number of them were measured with a Zeiss AIMS™ microscope to determine their lithographic significance.

For one particular 193 6% EPSM reticle, when inspected at full sensitivity with the TeraStar SLF27, 3 defects were detected. When inspecting with the TeraScan 525 at a de-sense setting, 40 defects were detected. Figure 4-10 shows the inspection difference images and AIMS measurements for several of the defects that were detected only by the 525. Based on the AIMS measurements, these defects may not be lithographically critical for the 90nm node, however, they likely would be lithographically significant for a smaller node. The higher sensitivity of the 525 will provide a way to make the necessary process improvements for the smaller nodes. A partial defect map in Figure 4-10, shows a row CD defects that suggest a process issue.

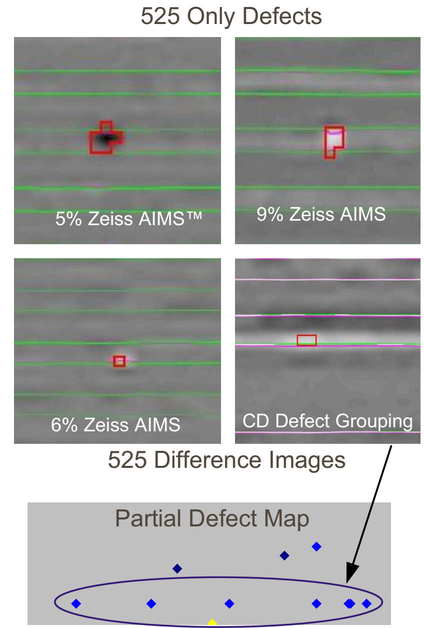

Figure 4-10: Defects Detected only by the 525 on a 90nm Node 193 6% EPSM Product Simulation Reticle

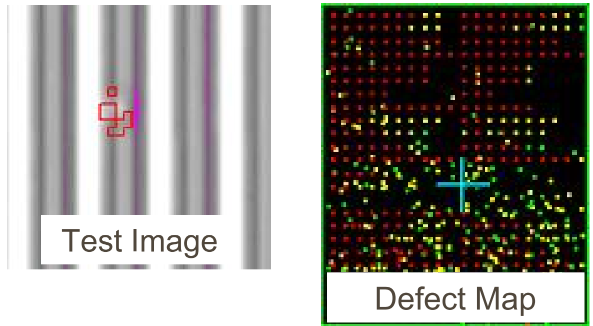

Figure 4-11: 75nm Node Chromeless Development Reticle Defect and Map Inspected with 525

Figure 4-11 shows the inspection result of a development 75nm node chromeless reticle provided by AMTC. This reticle was uninspectable with an SLF27 due to excessive false detections, whereas it was inspected properly by the 525 using the phase contrast mode. The defect count was high, however, upon examination, the defects detected were determined to be real. The 525 provided the necessary sensitivity to allow process improvement.

Figure 4-12 shows the inspection maps from a 65nm node 6% EPSM development reticle for 193 lithography contributed by Texas Instruments. This reticle had a very high false detection count at full sensitivity when inspected with an SLF27 due to small SRAF (624 false detections, 4 real defects). When inspected with the 525 125 pixel, there were 0 false detections and 19 real defects detected, suggesting the 125 pixel may be suitable for some types of 65nm node reticles.

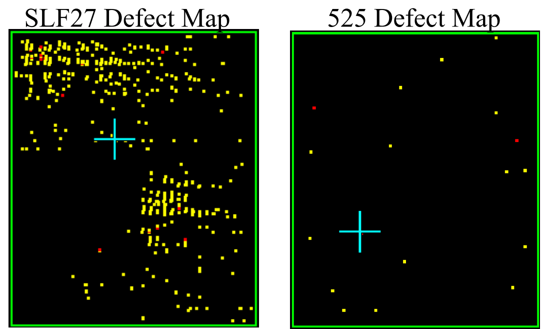

Figure 4-12: 65nm Node EPSM Development Reticle with Small SRAF - SLF27 with Excessive False Detections

Downloaded From: http://proceedings.spiedigitallibrary.org/ on 05/06/2014 Terms of Use: http://spiedl.org/terms

Figure 4-14 shows an undersize contact (6% flux) detected by the 525 125 pixel on a 65nm node development EPSM reticle contributed by Texas Instruments. This reticle contained various hole sizes, styles, spacings, and SRAF. The 525 inspected the reticle with low false detections and found important defects to help process improvement.

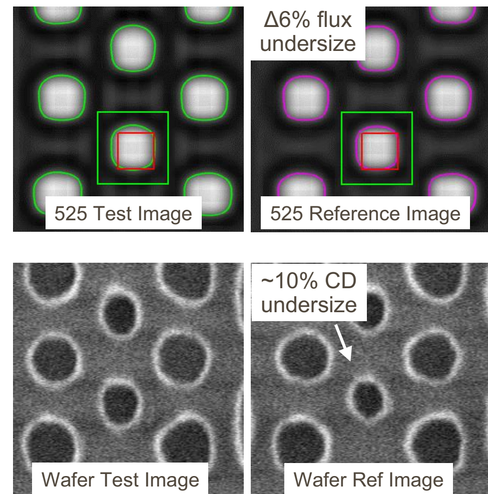

Figure 4-14: Undersize Contact (6% flux) Detected by the 525 from a 65nm Node Development Reticle

Figure 4-15: Crystal Defect Visibility SLF27 vs. 525 Showing Higher 525 Visibility

Figure 4-15 shows the higher sensitivity of the 525 imaging for crystal defects as compared to the SLF27 imaging. These images were taken from a 6% EPSM reticle used in 193 lithography as contributed by a wafer fab. The SLF27 could only find a small number of the larger crystals, whereas, the 525 found a large number of smaller crystals giving the opportunity to detect the crystals before they print.

4.4. Industry Product Reticle Test Observations

There were several notable observations from the testing done with the industry provided reticles.

First, the 525 had very low false detections (where a false detection is a system issue such as alignment, noise, vibration, etc.).

Second, the 525 had noticeably higher sensitivity than the SLF27 and often showed high numbers of small defects on reticles that had previously passed a full sensitivity SLF27 inspection. Since the defect level of a reticle manufacturing process is limited by the inspection system's ability to find defects, the higher sensitivity of the 525 can allow further reductions in defect levels for the smaller nodes. While many of the small defects detected by the 525 on today's 90nm reticles may be judged as not lithographically significant, many that were evaluated were close to the typical 10% CD guideline, causing some concern. The 525 further demonstrated much higher visibility of crystal defects compared to the SLF27 giving the opportunity to detect these defects before they print.

Finally, the 90 pixel was shown to have even more sensitivity suggesting good capability for the 65nm node.

5. Lithographic Detector Results

5.1. Defect Major Classes

Historically, defect repair has been effective, easy, and economical, so it was sufficient to simply classify defects by size and type to facilitate repair and process control (i.e. 100nm dark extension, or 110nm clear corner, etc,). However, in recent years, defect repair of high performance reticles has become less effective (possible damage), difficult (PSM

Downloaded From: http://proceedings.spiedigitallibrary.org/ on 05/06/2014 Terms of Use: http://spiedl.org/terms

reticles, CD defects), and the reticles themselves have become very expensive. So, rather than scrapping an expensive reticle due to an unrepairable defect, or risk damaging it with a tricky repair, reticle manufacturers and users are both asking if the defect really needs to be repaired, i.e. does it matter? In the end, a reticle defect is really only important if it affects the performance, yield, or reliability of the finished device. For a reticle manufacturer to quickly assess the eventual device impact of a reticle defect when deciding to pass, repair, or scrap the reticle is currently very difficult. KLA-Tencor is developing the technology to provide the key information at the decision point so a more informed quick decision can be made. Two key pieces of information are whether the defect is lithographically significant, and second, whether it is located in a part of the circuit that might affect device performance, yield, or reliability. This section discusses some early work that KLA-Tencor is doing to identify the lithographically significant defects; work in device significance will not be discussed here.

As mentioned, reticle defects that do not create an artifact in the etched wafer are typically not important to the wafer lithographer (didn't print). Therefore, if the inspection system can be designed to bin defects according to their likelihood of printing, this would reduce unneeded repairs, or unnecessary scrap, thus improving reticle yield and cycle time. A general rule is that a reticle defect is lithographically significant when it would impact the wafer linewidth by more than 10% (some wafer fabs are proposing much tighter rules especially for contact layers).

Conversely, a defect occurring during reticle manufacturing that is not likely to print, may not be important to the wafer lithographer, but is often important to the reticle manufacturer and reticle purchaser as one measure of reticle quality and the level of process control. These :"process defects" may be an indication of an impending process failure and should be identified and tracked, although they may not need to be repaired.

Similarly, reticle defects that occur during use (i.e. crystal growth, haze, ESD, etc) are of great interest to the lithographer because they can cause catastrophic yield loss if they print sufficiently in a critical location. These defects often grow larger with use so it is critical to detect them well before they print rather than after when it might be too late. These "progressive" defects have become much more problematic in advanced wafer fabs and must be guarded against.

5.2. Lithographic Detectors

The traditional defect detectors are designed to detect defects based on their size only according to the traditional definition of a defect. The detectors have been designed to be largely independent of the location, class, or type of the defect, thus generally finding any defect located anywhere. This location independence is typically accomplished by examining one small part of the geometry at a time without much regard to the surrounding geometry. Thus, for best performance, these traditional detectors use high resolution images so that all the details about the geometry are available. Figure 5-1 shows several small defects in different locations with progressively smaller geometry size (upper left to lower right). In general, a high resolution defect detector will detect all of these defect types equally based on their size.

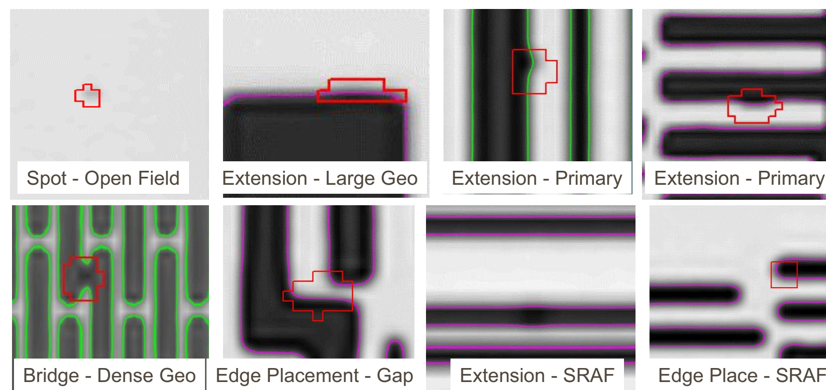

Figure 5-1: Defects on Progressively Smaller Geometry - traditionally detected with equal sensitivity based on defect size

Downloaded From: http://proceedings.spiedigitallibrary.org/ on 05/06/2014 Terms of Use: http://spiedl.org/terms

However, from a lithographic viewpoint, these defects have varying significance; the same size defect in each location has a different lithographic impact. Thus, a "lithography oriented detector" might be designed to have a different defect sensitivity depending upon the size and surrounding location of the defect - a small open field defect doesn't need to be detected, however, the same small defect in dense geometry does need to be detected.

Figure 5-2 shows the same defects as before (Figure 5-1), but graded by the detector sensitivity likely needed. If one were to simply follow a %CD rule for the defect size to be detected, the required sensitivity must clearly vary with the geometry size. However, in low k1 lithography, the required sensitivity may also need to vary according to the mask enhancement factor (MEF) which can itself vary from below 1, to 3 or 4, depending upon the characteristics of the target lithography. An interesting case is the sub-resolution assist feature (SRAF) which, although small, is not designed to print, therefore, from a lithographic viewpoint, small defects are less important (except for oversized SRAF which can catastrophically print and must be guarded against). Since SRAF are very challenging to the reticle manufacturing process, local CD errors are often an issue which must be guarded against through careful inspection.

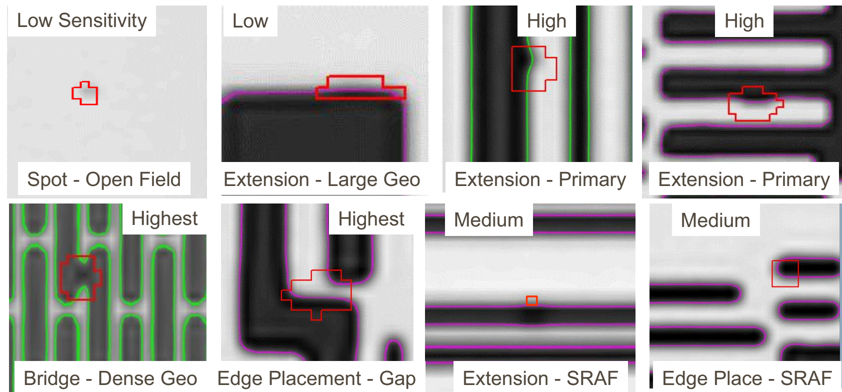

Figure 5-2: Defects on Progressively Smaller Geometry - graded by required sensitivity according to lithographic significance

To respond to the lithographic significance of defects, KLA-Tencor has developed defect detectors that are "lithography oriented" for the purpose of detecting and binning those defects that are likely to be lithographically significant. In addition, the existing high resolution detectors are used in parallel to detect and bin those defects that are significant to the reticle manufacturing process (process defects). By binning defects into either category, the user has new information to more effectively disposition detected defects according to significance (lithographic or process).

To better understand the design of the defect detectors, Figure 5-3 shows the conceptual image processing for the high resolution detectors (HiRes). Starting from the left, the high resolution images contain all of the details about the geometry and the defect. In this case, the test and reference images are shown with one of the images containing a clear spot defect (pinhole) - note that an edge outline is drawn artificially for easier viewing. When the two images are overlayed (differenced), the matching geometry becomes gray while the defect alone becomes separately visible (white or black indicates a difference between test and reference). A cross section through the difference image is shown next which indicates a reasonably strong signal from the defect. This defect signal is applied to a user adjustable double-sided thresholds (dotted lines) - signal beyond the threshold is detected as a defect, signal within is ignored. The thresholds can be used adjusted to be very tight (100), or very loose (1). Since defect detection is done with high resolution images, all structures of the geometry are examined for defects, both the primary geometry and the secondary sub-resolution geometry (e.g. serifs, jogs, and SRAF).

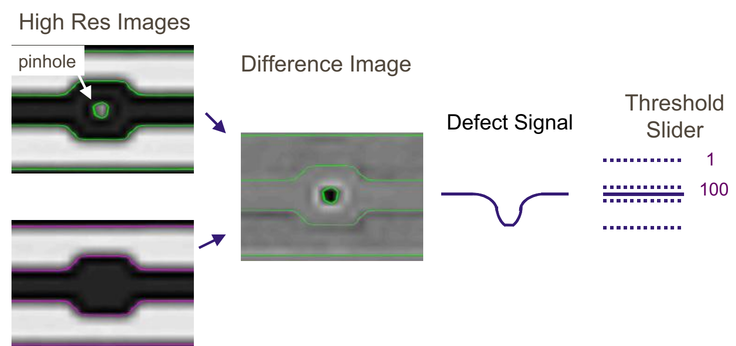

Figure 5-3: High Resolution Detectors Conceptual Image Processing

Downloaded From: http://proceedings.spiedigitallibrary.org/ on 05/06/2014 Terms of Use: http://spiedl.org/terms

Figure 5-4 shows the conceptual image processing for one type of lithographic detector (Litho1); other detectors have similar processing. The same high resolution images are used for the Litho detectors as for the HiRes detectors which allows the two types of detectors to operate in parallel. For the Litho1 detector, the high resolution images are first digitally filtered using a simple aerial image and resist model to produce the Litho Images. Note, that after digital filtering, the clear spot defect is barely visible, suggesting little lithographic impact. The two Litho images are then overlayed (differenced) to produce the Difference Image wherein matching geometry becomes gray and defects become white or black. The defect cross section shows very little signal, thus, it would only be detected by the Litho1 detector if the thresholds were very tight. Hence, only a much larger defect of this type in this location would be lithographically significant For the Litho1 detector, a separate MEF Analyzer has been added which can provide dynamic control of the threshold according to the local MEF, thus giving the user additional adjustment and control This first implementation of Litho detectors uses simple aerial image and resist models and does not allow direct input of the lithography parameters Selection of settings is done empirically using appropriate test reticles with programmed defects and their corresponding Zeiss AIMS reading or wafer print reading.

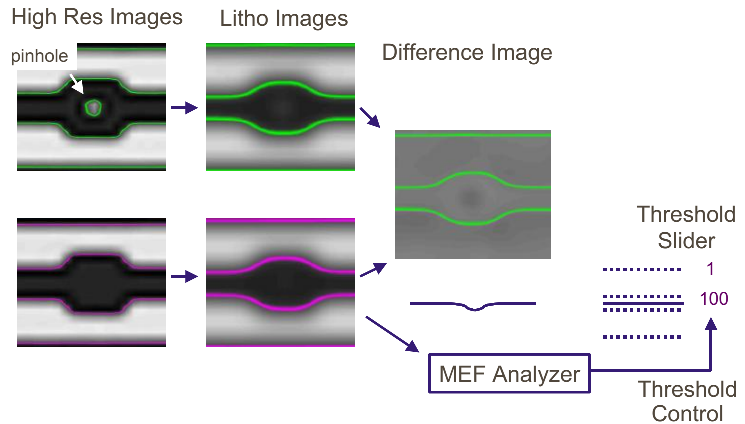

Figure 5-3: Lithography Oriented Detector Conceptual Image Processing

While the overlay method of defect detection is conceptually simple, it can be very challenging. To achieve both high sensitivity and low false detections over a large inspection area requires any residual optical, mechanical, sensor, and electronic errors in the image acquisition hardware to be minimized (e.g. vibration, optical distortion, illumination errors, etc.). These acquisition errors can create small overlay errors in very high populations which must then be ignored. Similarly, small errors in the reticle manufacturing equipment and process can also create small size high population overlay errors from the reticle which can further reduce overall sensitivity since they must be ignored (e.g. shot errors, proximity errors, edge roughness, butting errors, chemistry, etc.). Thus, very tight tolerances must be designed and maintained for the image acquisition hardware to minimize these types of errors, and the errors in the reticle manufacturing process must be consistent with the defect sensitivity wanted. Finally, sophisticated alignment and overlay algorithms must be employed to reject any remaining errors.

Last year, KLA-Tencor implemented TeraFlux for the TeraStar UV reticle inspection system as the first lithography oriented defect detector. TeraFlux was in response to numerous fabs experiencing closed or undersized contacts and vias on their wafers due to very small reticle defects. Since the MEF is often very high on hole layers (contacts and vias), significantly smaller reticle defects must be detected than are typically specified. Moreover, the types of defects were also important - a small two-sided or four-sided undersize CD defect was very important since it could significantly reduce the energy or flux through a contact, whereas a singular small edge extension might have little impact on the overall flux. This was further complicated by the limitations of typical reticle manufacturing processes in use, which could produce these high MEF unrepairable defects. TeraFlux was designed to detect small flux errors in the contacts, thus naturally detecting highly printable CD defects and suppressing sensitivity to small extension defects which have little flux impact. Referring back to Figure 4-3, the defect shown on the Cetus test reticle is a four-sided approximately 12nm CD defect on a 600nm contact that produces a 4% flux error - in some wafer processes this defect can be highly printable (see also Figure 4-14). Field testing of TeraFlux has shown the ability to readily detect these lithographically significant flux defects on hole layers, thus providing the necessary protection against repeating defects of this type. In addition, TeraFlux has allowed visibility of this type of defect at the reticle manufacturer, thus allowing changes in the reticle manufacturing process to reduce defect occurrence and thus improve reticle yield and cycle time.

The second implementation of lithography oriented detectors is the Litho1 and Litho2 detectors for the TeraScan 525. The Litho1 detector has basic capability and is designed for line/space and hole layers, while Litho2 is similar to

Downloaded From: http://proceedings.spiedigitallibrary.org/ on 05/06/2014 Terms of Use: http://spiedl.org/terms

TeraFlux and is designed for highest sensitivity on hole layers. KLA-Tencor is further designing a Litho3 detector which offers more accuracy and improved ease of use.

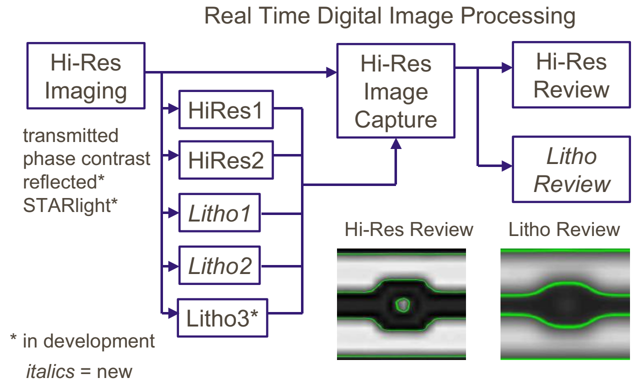

Figure 5-5: TeraScan Data Flow Diagram

Figure 5-5 shows a basic Data Flow Diagram of the TeraScan system. Starting from the left, the Hi-Res Imaging block consists of the Image Acquisition Subsystem which provides the high resolution images used by the defect detectors; the images are currently available in transmitted illumination with either standard contrast or phase contrast - reflected light and STARlight illumination modes are currently in development. To provide the best defect visibility, one or more of these illumination modes may be used according to the reticle type and defect type being inspected. All subsequent processing steps are done with real time digital image processing techniques. As shown, the different detectors all operate in parallel from the same high resolution images. When a defect is detected by any of the detectors, a high resolution image of the defect is captured. The user may adjust the settings for each detector individually to obtain the desired sensitivity for each detector. After defects are detected, the user can review the defect's original high resolution image to assess the nature and possible cause of the defect, and the user can also assess the defect based upon a lithographic view. Note that the Litho3 detector is currently in development.

5.3. Lithographic Detector Example

A simple example showing the use and benefit of the Litho1 detector and the HiRes detectors is described in this section. A 90nm node 193 6% EPSM programmed defect reticle was provided by a reticle manufacturer. In one section of the reticle, the background geometry was a 1:1 pitch line/space pattern representative of the 90nm node; it contained programmed defects of various sizes and types with an accompanying alpha-numeric identifier. In addition to the programmed defects, there were a variety of naturally occurring defects both in the dense line/space pattern and larger linewidth alpha-numeric pattern.

Preferably, AIMS or wafer print data of the programmed defects would be used to adjust the Litho1 detector, however, in this case, there was no data, so the settings for a typical 90nm lithography process were used. The HiRes detectors were adjusted to detect a moderate number of the naturally occurring process defects.

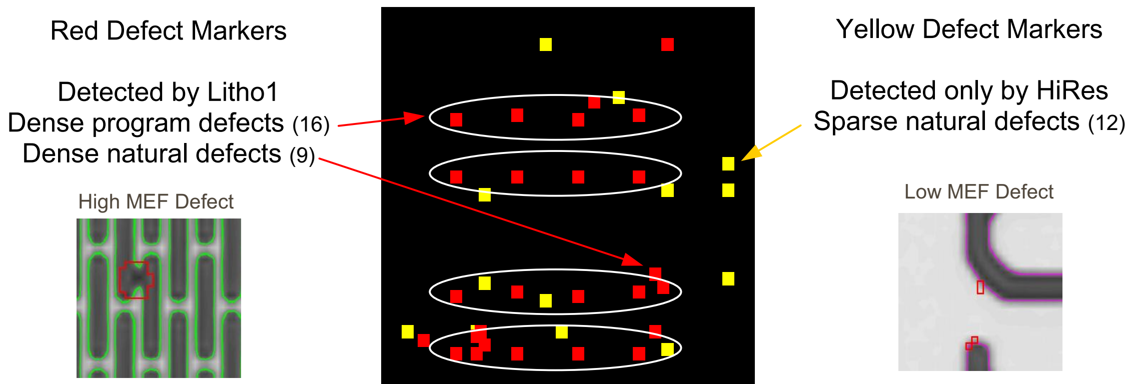

Figure 5-6: Lithographic Detector Simple Example

Figure 5-6, shows a small section of the resulting defect map. The red defect markers are those defects detected by the Litho1 detector and which are likely to be lithographically significant; note that they may also have been detected by one or both of the HiRes detectors, but are binned to Litho1 which has the highest priority. The red markers consist of the on-grid programmed defects in the dense line/space pattern (16ea as indicated), as well as the off-grid naturally

Downloaded From: http://proceedings.spiedigitallibrary.org/ on 05/06/2014 Terms of Use: http://spiedl.org/terms

occurring defects that are likely to be lithographically significant (9ea as indicated). The 12 yellow markers are those defects that were only detected by the HiRes1 detector (not detected by the Litho1 detector); there could also be green markers which would have been detected by the HiRes2 detector (none shown). The yellow markers are naturally occurring defects either in the larger geometry alpha-numerics or surrounding region which are typically low MEF areas and not likely to be lithographically significant Overall, the likely lithographically significant defects were binned to the Litho1 detector, while the defects unlikely to be lithographically significant were binned to the HiRes detector. In this way, the user has important additional information to appropriately disposition these defects.

This same type of experiment was repeated with several product reticles from several reticle manufacturers and showed interesting results. Typically a "good" 90nm node reticle was provided - the reticle had typically been inspected by a current generation TeraStar SLF27 with maximum sensitivity and had very few defects. When inspected with the TeraScan 525 HiRes detectors, a high population of small "process" defects was detected. Upon initial examination, many of the defects were on large geometry in low MEF areas and were typically judged to have little lithographic significance. Notwithstanding, due to the high population of defects, it would have been very time consuming to review each defect to ensure that all the defects were in low MEF areas, so this was not done.

Then, the Litho1 detector was enabled and adjusted for a typical 90nm node lithography process to see if there were any lithographically significant defects present among the high population of small "process" defects. Also, the HiRes detectors were set to less sensitive settings to reduce the number of process defects detected. After re-inspection, an alarming number of the small "process" defects previously detected were also detected by Litho1 since they were located in high MEF areas - several of these were later evaluated using a Zeiss AIMS microscope and confirmed to be lithographically significant.

So, several things were learned - first, the '"process" defects associated with the current 90nm reticle process are typically not lithographically significant when located in low MEF areas, but can be lithographically significant when located in high MEF areas. Second, the SLF27 is not capable of finding these small defects in either the low MEF or high MEF areas. Third, the 525 is capable of finding these small defects and can typically separate the low MEF process defects from the high MEF lithography defects by using the Litho1 detector and HiRes detectors appropriately set

6. Conclusions

A new DUV high-resolution reticle defect inspection platform has been developed to meet the sub-90nm node 248/193nm lithography reticle qualification requirements of the IC industry. The prototype and the first two beta systems have been tested in die-to-die mode using approximately sixty advanced reticles provided by the industry. These reticles represent primarily the 90nm node, but also early reticles down to the 65nm node. These reticles included COG, EPSM, and altPSM, with various OPC styles (serif, jog, and SRAF). Programmed defect types and regular full field product reticles were inspected. Data from the testing showed that the system met its sensitivity and false detection targets - selected supporting data was shown in this paper.

The higher sensitivity of the TeraScan 525 has shown the defect limitations of the current 90nm node reticle manufacturing processes. In these processes, there is typically a high population of small defects present which were not detectable with previous generation equipment. The visibility of these defects will now allow process improvements to enable the next nodes.

The design and early test results of the new lithography oriented detectors were shown. These detectors are designed to provide high sensitivity to those defects that are likely to have lithographic significance, while providing lower sensitivity to those defects with likely little lithographic significance. When used in conjunction with the traditional high resolution detectors, the user can readily identify those defects with likely lithographic significance requiring repair (or scrap), and those defects that are likely not lithographically significant but still important for reticle process monitoring and improvement.

The TeraScan platform includes several inspection modes, including die-to-die (discussed in this paper), die-to-database mode, and STARlight mode, the latter two are in development. In this paper, early data was shown for the die-to-

Downloaded From: http://proceedings.spiedigitallibrary.org/ on 05/06/2014 Terms of Use: http://spiedl.org/terms

database mode, and also for the new 90nm pixel which provides greater sensitivity and smaller linewidth capability for the aggressive reticles for the sub-90nm nodes.

7. Future Work

There are several new capabilities which are currently in development for the TeraScan platform. Future work will include testing these capabilities. They include:

- 90nm pixel for smaller linewidth and higher sensitivity
- die-to-database mode
- Litho3 detector for improved accuracy and ease of use
- reflected light mode die-to-die and die-to-database
- STARlight mode
- tri-tone die-to-database mode
- Zeiss AIMS interconnectivity

Acknowledgements

The authors thank the many individuals and organizations that contributed to the development and testing of the TeraScan 525, including:

- International SEMATECH for Tera Family and AltPSM funding
- Intel Mask Inspection Team for providing reticles
- Dr. Jan Heumann, AMTC for providing reticles and data
- Dr. Won Kim, Texas Instruments for providing reticles and data
- Worldwide reticle manufacturers and fabs for providing reticles used in development and testing
- KLA-Tencor RAPID Applications Team for data collection and analysis
- KLA-Tencor TeraScan Development Team for platform development

Downloaded From: http://proceedings.spiedigitallibrary.org/ on 05/06/2014 Terms of Use: http://spiedl.org/terms